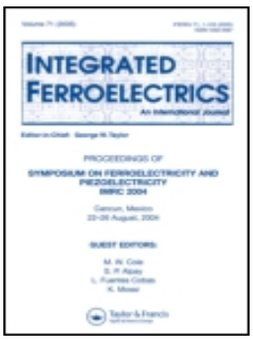

Integrated Ferroelectrics

An International Journal

ISSN: 1058-4587 (Print) 1607-8489 (Online) Journal homepage: https://www.tandfonline.com/loi/ginf20

Ferroic properties of $0.675[Pb(Mg_{1/3}Nb_{2/3})O_3]-0.325[PbTiO_3]/CoFe_2O_4$ prepared by spark plasma sintering

D. S. F. Viana, F. P. Milton, K. R. C. P. Jimenez, A. J. Gualdi, P. C. Camargo, A. J. A. de Oliveira, J. A. Eiras, A. Bhalla, R. Guo & D. Garcia

To cite this article: D. S. F. Viana, F. P. Milton, K. R. C. P. Jimenez, A. J. Gualdi, P. C. Camargo, A. J. A. de Oliveira, J. A. Eiras, A. Bhalla, R. Guo & D. Garcia (2016) Ferroic properties of $0.675[Pb(Mg_{1/3}Nb_{2/3})O_3]-0.325[PbTiO_3]/CoFe_2O_4$ prepared by spark plasma sintering, Integrated Ferroelectrics, 174:1, 138-145, DOI: 10.1080/10584587.2016.1194679

To link to this article: https://doi.org/10.1080/10584587.2016.1194679

Published online: 13 Jul 2016.

INTEGRATED FERROELECTRICS
2016, VOL. 174, 138–145
http://dx.doi.org/10.1080/10584587.2016.1194679

Taylor & Francis
Taylor & Francis Group

Ferroic properties of $0.675[Pb(Mg_{1/3}Nb_{2/3})O_3]-0.325[PbTiO_3]/CoFe_2O_4$ prepared by spark plasma sintering

D. S. F. Viana[a,b], F. P. Milton[a], K. R. C. P. Jimenez[a], A. J. Gualdi[a], P. C. Camargo[a], A. J. A. de Oliveira[a], J. A. Eiras[a], A. Bhalla[b], R. Guo[b], and D. Garcia[a]

[a]Physics Department, Federal University of São Carlos, São Carlos, SP, Brazil; [b]Multifunctional Electronic Materials and Devices Research Lab, College of Engineering, University of Texas at San Antonio, San Antonio,TX, USA

ABSTRACT

This paper reports the electric, magnetic and magnetoelectric properties of particulate composites of the system with ferroelectric phase $0.675[Pb(Mg_{1/3}Nb_{2/3})O_3]-0.325[PbTiO_3]$ and magnetic phase $CoFe_2O_4$ prepared by Spark Plasma Sintering technique. Optimized sintering and thermal annealing parameters were applied in order to achieve highly dense microstructure with sub micrometric grain size distribution for both phases. The results from the dielectric measurements showed a diffuse and dispersive phase transition. P-E and M-H loops revealed the simultaneous existence of ferroelectric and ferrimagnetic ordering, respectively. Moreover, at cryogenic temperatures an anomalous behavior on the bias magnetic field dependence was observed for the magnetoelectric voltage coefficient.

ARTICLE HISTORY
Accepted 15 January 2016

KEYWORDS
Magnetoelectric effect; magnetoelectric composites; Spark Plasma Sintering

Introduction

The presence of more than one ferroic property in a single material has drawn an ever increasing interest upon multiferroics, given their considerable potential for practical applications [1–3]. The coupling of magnetic and electric properties, known as the magnetoelectric (ME) effect, wherein a magnetic field can induce an electric polarization and an electric field can induce a magnetization, offers new technological possibilities [2–4], such as magnetic sensors for dc or ac magnetic fields, transducers or actuators [5–7]. In the case of composite materials, the ME effect arises from the magnetic-mechanical-electric interactions between the magnetostrictive and piezoelectric phases [8].

The occurrence of magnetoelectric effect has already been reported in composites of $CoFe_2O_4$ (CFO) with the morphotropic phase boundary (MPB) composition $0.675[Pb(Mg_{1/3}Nb_{2/3})O_3]–0.325[PbTiO_3]$ (PMN-PT), prepared by various methods such as the conventional sintering method [9], hot forging [10] and thin films

CONTACT D. S. F. Viana diegoseiti@hotmail.com

(heterostructures) [11]. However, studies for PMNPT/CFO particulate composites prepared by the Spark Plasma Sintering (SPS) are yet to be conducted.

It is known that the ME response in composites can be strongly affected through the variation of composition, microstructure (as grain size, shape and orientation) and sintering parameters [8]. Therefore, the commonly high-dense and fine-grained samples obtained by SPS technique could possibly provide unusual magnetoelectric responses.

Although there are several reports on the effect of grain size upon piezoelectric, dielectric and ferroelectric properties [12–14], the effect upon magnetoelectric properties has not been well reported. In the case of morphotropic phase boundary $0.675[PbMg_{1/3}Nb_{2/3}O_3]–0.325[PbTiO_3]$ ceramics, smaller grain size may induce a dielectric relaxor behavior instead of a normal dielectric response. In addition, it is known that the electric field dependence of the piezoelectric/electrostrictive strain changes if the grain size changes from micrometers to nanometers [14]. Since in ME composites strain plays a main role in mediating the magnetoelectric coupling, particulate composites with smaller grain sizes (nm order) in the ferroelectric phase could produce a different magnetoelectric response from those in which average grain size is in the micrometer order.

This paper reports on the ferroic properties of the magnetoelectric particulate composite (0.8)[0.675PMN-0.325PT]/(0.2)CFO with average grain size of 230 nm for the ferroelectric phase and 250 nm for the ferrite phase. The powders were prepared by the solid-state reaction and sintered by the Spark Plasma Sintering technique.The dielectric behavior, polarization vs electric field and magnetization vs magnetic field dependence were also assessed. Measurements of magnetoelectric voltage coefficient at several temperatures were carried out in the 50 K – 300 K temperature range.

Experimental procedure

The powders of the (0.675)PMN–(0.325)PT and $CoFe_2O_4$ systems were separately synthesized by the solid-state reaction method. In order to reduce the particle size, the PMN-PT powders were wet ball milled with 1 mm diameter zirconia balls as grinding media, at 170 rpm, for 24 h, followed by another 24 h milling with 0.5 mm diameter zirconia balls, and dried. The proportion of 80 and 20 mol % of PMN-PT and CFO, respectively, was blended in a planetary ball mill at 300 rpm for 1 h. The blended powders were heated at 800°C for 5 min under argon atmosphere in a Spark Plasma Sintering System (Dr. Sinter model, Sumitomo Co). Annealing under the optimized conditions of 24 h at 690°C and PbO atmosphere was done for the sintered samples, following post-sintering thermal treatment protocol, which details are previously reported in the ref.[15]. Phase identification was performed through X-ray diffraction (XRD) analysis using Rigaku Rotaflex RU200B powder diffractometer, with CuKα radiation and 2θ from 10–60, 2°/min. The apparent density was obtained by the Archimedes method, with distilled water as immersion liquid. Computer-assisted dielectric measurements were carried out during heating run

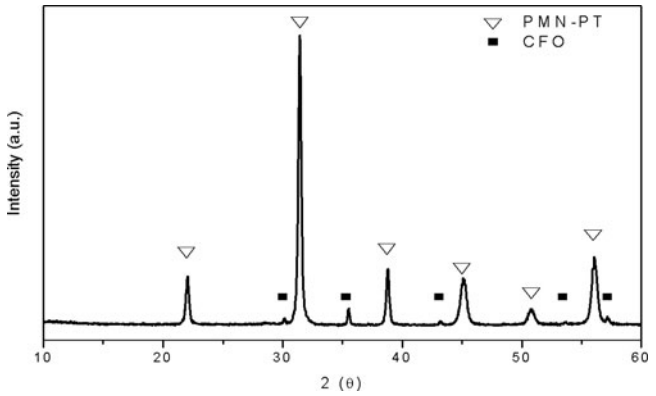

Figure 1. XRD patterns of the magnetoelectric composite 0.8 PMN-PT/ 0.2 CFO prepared through the Spark Plasma Sintering method.

(2 K/min) using a HP4194 Impedance-Gain Phase Analyzer coupled to a home-made furnace. The electrical characterization was performed on the ceramics using a model 617Keithley multimeter. Ferroelectric hysteresis loops were assessed with a modified Sawyer–Tower circuit.The magnetic measurements were performed using a Quantum Design Squid-VSM magnetometer. The magnetoelectric measurements were performed in the Physical Properties Measurement System (PPMS-6000).

Results and discussion

Figure 1 shows the room temperature X-ray diffraction powder profiles for the (0.8)[0.675 PMN-0.325 PT]/(0.2)CFO particulate composites prepared by the SPS process. These XRD profiles showed the peaks corresponding to the spinel CFO phase and the perovskite PMN-PT phase without traces of any spurious compounds. The XRD peaks of the perovskite phase belongs to a PT concentration that lies in the PMN-PT morphotropic phase boundary region [16,17] in agreement to the composition of the batch formula.

Average particle size was 210 nm for the as-calcined CFO powder and 150 nm for the calcined and ball-milled PMN-PT powder. After the sintering process and thermal treatment in a rich PbO environment, the average grain size was 230 nm for the ferroelectric phase and 250 nm for the magnetic phase, as previously reported by the authors [15]. In comparison with conventional methods [16,17], the faster firing and lower sintering temperature enabled by the SPS system were the key for the grain growth control on these composites.The sintering and thermal treatment protocols allowed obtaining bulk particulate composites with high density (98% of the calculated density) and relatively high electrical resistivity ($\sim 10^7 \Omega$m). The resistivity values are similar to those found in similar composites by other researchers [18].

Figure 2 shows the temperature dependence of the real (ε') and imaginary (ε") dielectric permittivity at several frequencies in PMNPT/CFO. The value of dielectric permittivity obtained at 1 kHz and room temperature was 781.This value was smaller than that of 1241 observed by Mathe et al. [19], although it could be due

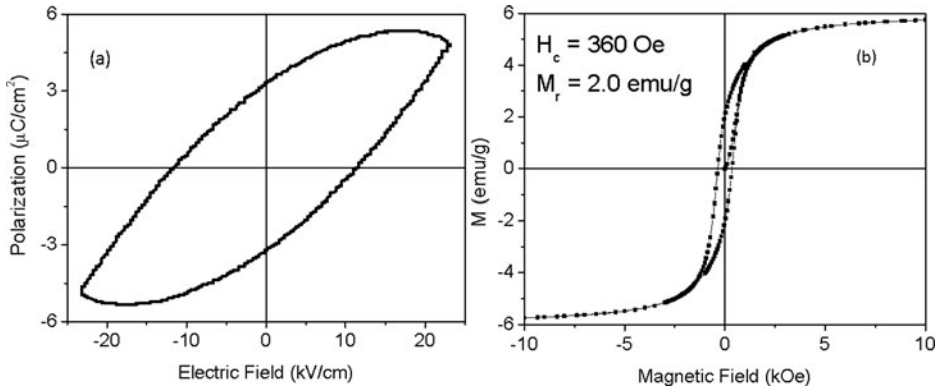

Figure 2. Temperature and frequency dependence of the real (ε') and imaginary (ε'') components of the relative permittivity. The frequencies measured were 0.1, 0.3, 0.5, 0.7, 1, 3, 5, 7 and 10 kHz.

to the different average grain sizes existing in the sample studied herein. Likewise the value measured for the dielectric loss at 1 kHz and room temperature was lower than that reported in ref. [19], 0.15 vs. 0.18.

A frequency dispersion of the maximum value of real permittivity was observed wherein increasing the frequency shifting the dielectric maxima to higher temperatures, as one can see in figure 2 (a).In addition, it is possible to see the contribution of dc conductivity increasing with the temperature as shown clearly in ε" vs. temperature plots, figure 2 (b). The relatively high dielectric permittivity values at lower frequencies could also be associated with the conductivity of the ferrite phase, with heterogeneous conduction [18] and sometimes with the polaron hopping mechanism, resulting in electronic polarization and contributing to more pronounced low frequency dispersion [19]. This could also be partially attributed to Maxwell–Wagner [20,21] type interfacial polarization in agreement with Koop's theory [22]. Furthermore, this will also arise from the relaxor MPB composition PMN-PT nanosize powder and samples [24]. However, such relaxor behavior could be overshadowed by the presence of conductivity sources along with the nanoscale size effects in relaxors. In future works, such effects can be addressed and the effect of each on the composite measurements will be analyzed and separated.

Electric and magnetic measurements were performed and the corresponding hysteresis loops are shown in figure 3 (a) and (b), respectively. The electric hysteresis loop was recorded at room temperature at a frequency of 50 Hz. The contribution of conductivity to the ferroelectric hysteresis is noticeable from the rounded shape of the curve. The polarization value was smaller than that reported by other authors [24] but, to some extent, this decrease in electric polarization is expected due to the smaller average grain size of the ferroelectric phase in these composites. The magnetic hysteresis curve shown in figure 3(b) reveals the ferrimagnetic nature of the composite. The values of remanent magnetization are smaller than those reported for composites prepared through other methods. Different values of remanent magnetization and coercive field for the pure CFO are found in the literature. These differences also depend on the grain size, grain morphology, oxidation state of iron

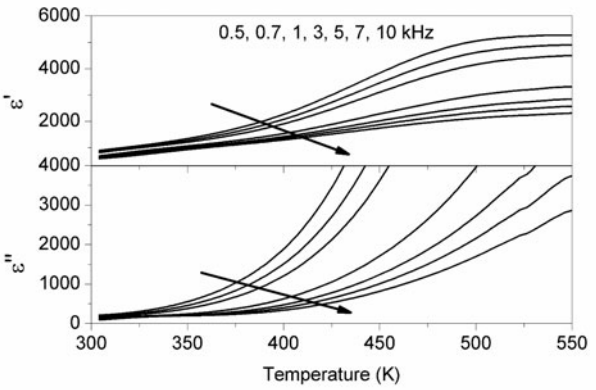

Figure 3. (a) Conductivity dominated Polarization vs Electric Field curve at 50 Hz at room temperature; (b) Magnetization vs Magnetic Field curve at room temperature.

(2+ and 3+), and cobalt, as these parameters are also linked with the preparation method [25–27].

Magnetoelectric measurements were performed in order to verify the coupling between the electric and magnetic properties. The sample was poled at 2 kV/mm for 30 min at room temperature and the measurements were carried out at the frequency of 1 kHz. Normalized magnetoelectric coefficient curves as a function of magnetic field for the composite at several temperatures are shown in Figure 4.

The evolution of the magnetoelectric coefficient with the temperature can be observed as well as a typical response for a magnetoelectric composite at 300 K [10]. At room temperature, the magnetoelectric coefficient reached the maximum value at a magnetic field of 4.9 kOe. The maximum of DC magnetic field maximum of magnetoelectric response for PMN-PT/CFO composites are found to be 1.3 kOe

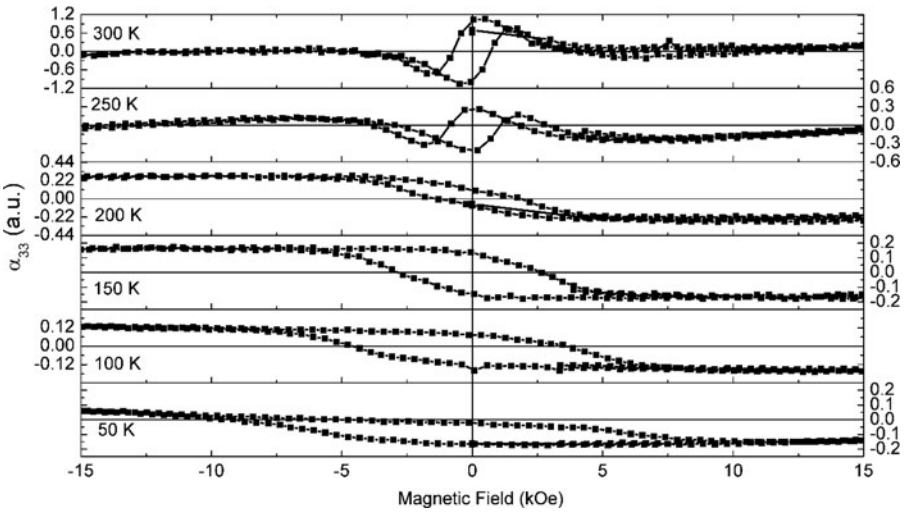

Figure 4. Normalized magnetoelectric coefficient at 1 kHz magnetic ac field and several temperatures of 0.8 (PMN-PT)/ 0.2 (CFO) poled at 2 kV/mm for 30 minutes at room temperature. The ME maximum occurs at 450 Oe at room temperature (300 K).

[10], 5.1 kOe [26] and 5.6 kOe [19] probably due to the fact that the microstructure (grain size, grain shape and degree of connectivity) may be different among samples from these different sources. As the temperature decreases, the value of the magnetoelectric coefficient also goes down. In addition, a change in the behavior of magnetoelectric coefficient as a function of the bias magnetic fiels appears at a temperature of 200 K where a hysteretic curve is observed. However, further studies are required to clarify the nature of this change in the magnetoelectric coefficient behavior and its relationship to any possible changes in the magnetic behavior of CFO.

Conclusions

Magnetoelectric particulate composites of 0.8(PMN-PT)/0.2(CFO), corresponding to a 77 : 23% volume ratio, with an average grain size of $\sim$ 200 nm for both phases and without the presence of any spurious phase were synthesized by the Spark Plasma Sintering method. Ceramic bodies with 98% of apparent relative density were obtained. Electric and magnetic hysteresis loops showed the existence of the electric and magnetic orders, and the magnetoelectric measurements confirm the presence of coupling between the two ferroic phases. The lower observed values of magnetization and electric polarization in these SPS ceramic composites could be due to the grain size effects and relatively high dc conductivity of the samples. Studies on various average grain sizes and volume fractions of the two components are in progress and the results will be published in upcoming papers.

Acknowledgements

To Mr. Francisco J. Picon (GCFerr), Mrs. Natália Ap. Zanardi (DF-UFSCar) and Mr. José A. L. da Rocha (IFSC-USP) for technical support. To Prof. Dr. Yvonne P. Mascarenhas (Crystallography Group of the IFSC-USP) for the access to the X Ray Diffraction facilities. To FAPESP (Proc. n. 2008/04025-0) and CAPES for the financial support. Authors also acknowledge the support of INAMM/NSF,the UTSA and W911NF-12-1-0082 grants.

References

1. N. A. Hill Why are there so few magnetic ferroelectrics?. *J Phys. Chem. B* **104**, 6694–6709 (2000).
2. W. Eerenstein, N. D. Mathur, J. F. Scott Multiferroic and magnetoelectric materials. *Nature* **442**, 759–765 (2006).
3. J. V. den Brink, D. I. Khomskii Multiferroicity due charge ordering. *J. Phys.: Condens. Matter* **20**, 1–12 (2008).
4. M. Fiebig Revival of magnetoelectric effect. *J. Phys. D. Appl. Phys.* **123**, R123–R 152 (2005).
5. K. H. Shin, M. Inoue, K. I. Arai Elastically coupled magneto-electric elements with highly magnetostrictive amorphous films and PZT substrates. *Smart Mater. Struct.* **9**, 357–361 (2000).

6. S. A. Wolf, D. D. Awschalom, R. A. Buhrman, J. M. Daughton, S. von Molnár, M. L. Roukes, A. Y. Chtchelkanova, D. M. Treger Spintronics: A spin-based electronics vision for the future. *Science* **294**, 1488–1495 (2001).
7. J. L. Prieto, C. Aroca, E. Lopez, M. C. Sanchez, P. Sanchez Magnetization processes and optimal performance of magnetostrictivepiezolelectric sensors. *J. Appl. Phys.* **79**, 7099–7105 (1996).
8. R. A. Islam, S. Priya Progress in dual (piezoelectric-magnetostrictive) phase magnetoelectric sintered composites. *Adv. Cond. Matter Phys.* **2011**, 1–29 (2011).
9. A. D. Sheikh, V. L. Mathe Composition dependent phase connectivity, dielectric and magnetoelectric properties of magnetoelectric composites with $Pb(Mg_{1/3}Nb_{2/3})(0.67)Ti_{0.33}O_3$ as piezoelectric phase. *Materials Research Bulletin* **44**, 2194–2200 (2009).
10. F. L. Zabotto, A. J. Gualdi, J. A. Eiras, A. J. A. de Oliveira, D. Garcia Angular dependence of the magnetoelectric effect on PMN-PT/CFO particulate composites. *Integrated Ferroelectrics: An International Journal* **131**, 127–133 (2011).
11. Z. Wang, R. Viswan, B. Hu, J-F. Li, V. G. Harris, D. Viehland Domain rotation induced strain effect on the magnetic and magneto-electric response in $CoFe_2O_4$/Pb(Mg,Nb)O_3-$PbTiO_3$ heterostructures. *J. Appl. Phys.* **111**, 034108 (2012).
12. B. S. Kang, D. G. Choi, S. K. Choi Effects of grain size on pyroelectric and dieletric properties of Pb0.9La0.1TiO3 ceramic. *J. Korean Phys. Soc.* **32**, S232–S234 (1998).
13. S. Choudhury, Y. L. Li, C. Krill, L. Q. Chen Effect of grain orientation and grain size on ferroelectric domain switching and evolution: phase field simulations. *Acta Materialia* **55**, 1415–1426 (2007).
14. Z-G. Ye Handbook of advanced dielectric, piezoelectric and ferroelectric materials synthesis, properties and applications 1st Edition. *Woodhead Publishing online* (2008).
15. D. S. F. Viana, J. A. Eiras, W. J. Nascimento, F. L. Zabotto, D. Garcia Controlled atmosphere thermal treatment for pyrochlore phase elimination of PMN-PT/CFO prepared by Spark Plasma Sintering. *Adv. Mat. Res.* **975**, 274–279 (2014).
16. J. C. Ho, K. S. Liu, S. J. Park Study of ferroelectricity in the PMN-PT system near the morphotropic phase boundary. *J. Mater. Sci.* **28**, 4497–4502 (1993).
17. J. Kelly, M. Leonard, C. Tantigate, A. Safari Effect of Composition on the Electromechanical Properties of (1-x)$Pb(Mg_{1/3}Nb_{2/3})O_3$−(X)$PbTiO_3$ Ceramics. *J. Am. Ceram. Spc.* **80**, 957–964 (1997).
18. Y. Zhi, A. Chen Maxwell-Wagner polarization in ceramic composites $BaTiO_3$-$(Ni_{0.3}Zn_{0.7})Fe_{2.1}O_4$. *J. Appl. Phys.* **91**, 794–797 (2002).
19. R. C. Kambale, P. A. Shaikh, Y. D. Kolekar, C. H. Bhosale, K. Y. Rajpure Studies on dielectric and magnetoelectric behavior of 25% CMFO ferrite and 75% BZT ferroelectric multiferroic-magnetoelectric composites. *Materials Letters* **64**, 520–523 (2010).
20. K. W. Wagner The theory of incomplete dielectricity. *Ann. Phys.* **40**, 817–855 (1913).
21. J. C. Maxwell *Electricity and Magnetism*. London: Oxford University Press; (1973).
22. C. G. Koops On the dispersion of resistivity and dielectric constant of some semiconductors at audiofrequencies. *Phys. Rev.* **83**, 121–124 (1951).
23. R. Zuo, T. Granzow, D. C. Lupascu, J. Rodel PMN-PT ceramics prepared by spark plasma sintering. *J. Am. Ceram. Soc.* **90**, 1101–1106 (2007).
24. A. D. Sheikh, V. L. Mathe Dielectric, ferroelectric, magnetic and magnetoelectric properties of PMN-PT based ME composites. *J. Phys. Chem. Solids* **72**, 1423–1429 (2011).
25. K. Vasundhara, S. N. Achary, S. K. P. Deshpande, P. D. Babu, S. S. Meena, A. K. Tyagi Size dependent magnetic and dielectric properties of nano $CoFe_2O_4$ prepared by a salt assisted gel-combustion method. *J. Appl. Phys.* **113**, 194101–194110 (2013).
26. B. G. Toksha, S. E. Shirsath, S. M. Patange, K. M. Jadhav Structural investigations and magnetic properties of cobalt ferrite nanoparticles prepared by sol–gel auto combustion method. *Solid State Communications* **147**, 479–483 (2008).

27. K. Maaza, A. Mumtaza, S. K. Hasanaina, A. Ceylan Synthesis and magnetic properties of cobalt ferrite (CoFe2O4) nanoparticles prepared by wet chemical route. *J. Magn. Magn. Mat.s* **308**, 289–295 (2008).
28. Y. I. Kim, D. Kim, S. L. Lee Synthesis and characterization of CoFe2O4 magnetic nanoparticles prepared by temperature-controlled coprecipitation method. *Physica B* **337**, 42–51 (2003).